Structural Engineering and Mechanics, Vol. 6, No. 3 (1998) 245-257
DOI: http://dx.doi.org/10.12989/sem.1998.6.3.245

Analysis and design of inclined piles used to prevent downhill creep of unsaturated clay formations

H.B. Poorooshasb †

Civil Engineering, Concordia University, Montreal, Canada

N. Miura ‡

Institute of Lowland Technology, Saga University, 1 Hanjo, Saga 840, Japan

Ali Noorzad ‡†

Concordia University, Montreal, Canada

Abstract. This paper present an analysis which may be used to obtain a rational design of a system of inclined piles used in preventing downhill creep of unsaturated clay formations. It uses two simple and relatively easy to measure parameters (an estimate of the maximum downhill creep together with a knowledge of the depth of the so called active zone) to calculate the required section size and the optimal spacing (pitch) of the piles for a desired efficiency of the system as a whole. Design charts are provided to facilitate the process.

Key words: saturated and unsaturated clays; downhill creep; piles; rainfall; pitch.

1. Introduction

This paper is an extension to an earlier work by the first author and his colleagues in Brazil (Poorooshasb, *et al.* 1988) who proposed an elementary method of analysis of inclined bamboo dowels to prevent the downhill creep of slopes consisting of unsaturated clays. Quite apart from the fact that the cited paper contained a mistake in logic, it suffered from two other constraints. It required a knowledge of the modulus of lateral reaction (a parameter very difficult to estimate) and it would not provide any information regarding the spacing of the piles (the pitch) in the system. Both these difficulties are overcome in the present paper by using a new analytical approach (called the ID technique since the procedure involves the evaluation of an Intergro-Differential equation) which was recently introduced (Poorooshasb, *et al.* 1996a, b) and applied to the examination of the performance of a system of vertical piles. The results of the analysis are

† Professor, Presently Guest Professor, ILT, Saga University, Japan
‡ Director
‡† Graduate Student, Presently Visiting fellow, ILT, Saga University, Japan

summarized in a number of design charts which may be employed directly.

This paper is written in the following sequence. First a brief literature review is presented. This is followed by a discussion of the nature of the creep under study. Next an outline of the ID technique *pertaining to the present situation* is provided together with the numerical scheme employed. Next the influence of various factors involved in the study (the angle of slope of the hill, the depth of the active zone, size and properties of the piles used and the spacing of the piles) on the overall performance of the system is examined. Finally the paper is concluded with three design charts for timber piles, concrete piles and H section steel piles.

2. Literature review

Stabilization of slopes using stiff piles, dowels or drilled shafts has been in usage in geotechnical engineering practice for some time. The reinforcement members are often driven or inserted vertically into the ground so as to intersect the potential failure surfaces and transfer the force from sliding mass on the stronger underlying strata. Most of the approaches presently available for the design of the stabilized slopes, are based on the limit equilibrium method.

Wang and Yen (1974) provide a solution for estimating the average soil pressure due to presence of piles in a slope and obtain an expression for the critical spacing of piles above which there is no arching. Ito and Matsul (1975) use the analogy of the extrusion of metals through dies and rollers, to estimate the pressure exerted on piles as the soil is squeezed through the space in between. The bending moment developed in the piles can be calculated according to Fukuoka (1975). Viggiani (1981) proposed mechanism for the yielding of the piles by the deformation of one or two plastic hinges. Guidelines for the analysis of drilled shafts for stabilizing slopes have been proposed by Reese, *et al.* (1992) while Pearlman, *et al.* (1992) describes the analysis of vertical and near vertical "pin piles". All these approaches deal with increasing the stability of the slope in terms of a factor of safety and designing the piles or drilled shafts to provide the required stabilizing force. Gudehus and Schwarz (1981) consider reduction of the creep rate of cohesive slopes consequent to the installation of vertical dowels. For calculating the reduction creep rate the soil is treated as viscous fluid while the dowel is analyzed as a flexible beam unrestrained at the top.

An alternative approach is soil nailing. The soil nail, typically a steel bar, is installed at various inclinations, the most preferred direction being the one orthogonal to the potential failure surface, The nail is duly bonded to the soil and improves the stability of the ground in the form of tensile reinforcement. The nails together with the in situ soil form a coherent structural mass that arrests the movement of an unstable slope. Gassler (1990) presents a detailed state of the art report for the design of soil nailing.

3. Cause and magnitude of the creep movement

Fig. 1 shows a portion of a slope of "infinite extent" with an active zone of depth z_0. Within the active zone the moisture content of the soil undergoes seasonal changes increasing its moisture content during the rainy season. At elevations below the active zone the water content of the soil remains unchanged. The variation of the moisture content within the active zone is associated with a softening of the material; that is, a marked reduction in the soil suction and con-

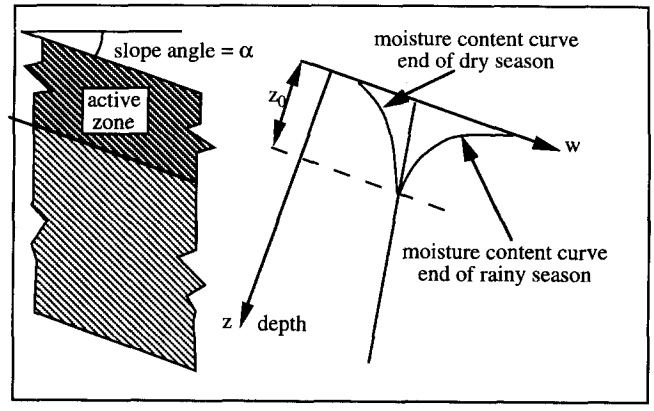

Fig. 1 Seasonal variation of moisture content with depth below surface of the slope.

sequently its shear modulus. Let the shear modulus and the unit weight of the soil at the end of the dry period be dented by G_d and γ_d respectively. Similarly let G_w and γ_w be the corresponding values at the end of the rainy season. It is easy to deduce that since $G_d > G_w$ and $\gamma_d < \gamma_w$ then downhill movement of magnitude u_s takes place such that:

$$\frac{du_s}{dz} = \frac{\gamma_w z \sin\alpha}{G_w} - \frac{\gamma_d z \sin\alpha}{G_d} \tag{1}$$

where z is measured from the surface as shown in Fig. 1. Near the surface the soil is fully saturated and furthermore since there are no overburden pressure the shear modulus of the soil approaches a negligible value. At depth z_0 the shear modulus is at its constant value of G_d. Thus it is logical to assume a variation of G_w with depth in the form;

$$G_w = \lambda z, \tag{2}$$

where λ, a constant, is given by the relation:

$$\lambda = \frac{G_d}{z_0} \tag{3}$$

It is difficult to estimate the value of λ (or G_d) which is required in the analysis. However its magnitude can be estimated from a knowledge of the total downhill creep. When G_w, as defined in Eqs. (2) and (3), is substituted in Eq. (1) and the results integrated the profile of the creep is obtained in the form;

$$u_s = \frac{(z - z_0)\sin\alpha}{\lambda z_0}\left[\gamma_w z_0 - \frac{1}{2}\gamma_d (z + z_0)\right] \tag{4}$$

At $z=0$ (i.e., on the surface) $u_s=\delta$, where δ is the maximum creep of the soil layer. Thus from the last equation the value of λ is obtained as;

$$\lambda = \frac{z_0 \sin\alpha}{\delta}\left[\gamma_w - \frac{1}{2}\gamma_d\right] \tag{5}$$

All quantities involved in Eq. (5) are now easily determined. Thus the evaluation of λ (and

hence G_w) is accomplished. Actually in the numerical application the expression used is $G_w = .00001 + \lambda z$ to prevent the division by zero error message.

4. Outline of the analytical procedure

Fig. 2 shows the right handed coordinate system used in this study. The origin of the coordinate system is taken at the center of a pile with the z axis along its center line. The x and y axes are assumed to pass through the center of the cross section of the adjacent piles. In this paper the pattern of installation is assumed to be square (i.e., the spacing downhill is assumed to be equal to the spacing across the hill) although this is not by any means a restriction that need be imposed in general. In view of the symmetry of the problem the solution region occupies only one half of the volume contained within the four neighboring piles as shown in the Figure.

The pivotal point in the analysis presented here is the following assumption; *for the type of problem considered the magnitude of the downhill movement of the soil is so large in comparison with the other components of the movement that the other components may be assumed to be negligibly small.* Thus if the movement along the x, y, z axes are denoted by u, v and w respectively then the fundamental assumption used in this paper states that;

$$u = u(x, y, z) \tag{6}$$

$$v = w = 0 \tag{7}$$

With this assumption it is easy to show that the following relations hold true:

$$\sigma_{xx} = \frac{2(1+\nu)G}{1-\nu-2\nu^2}\frac{\partial u}{\partial x}; \quad \sigma_{xy} = G\frac{\partial u}{\partial y}; \quad \sigma_{xz} = G\frac{\partial u}{\partial z} \tag{8}$$

where, ν is the Poisson ration of the soil (about 0.2 for most soils) and where the subscript w has been left out of the symbol representing the shear modulus in the set of Eqs. (8). Inserting the last set in the incremental equation of equilibrium in the x direction, that is, the equation:

$$\frac{\partial \sigma_{xx}}{\partial x} + \frac{\partial \sigma_{xy}}{\partial y} + \frac{\partial \sigma_{xz}}{\partial z} = 0$$

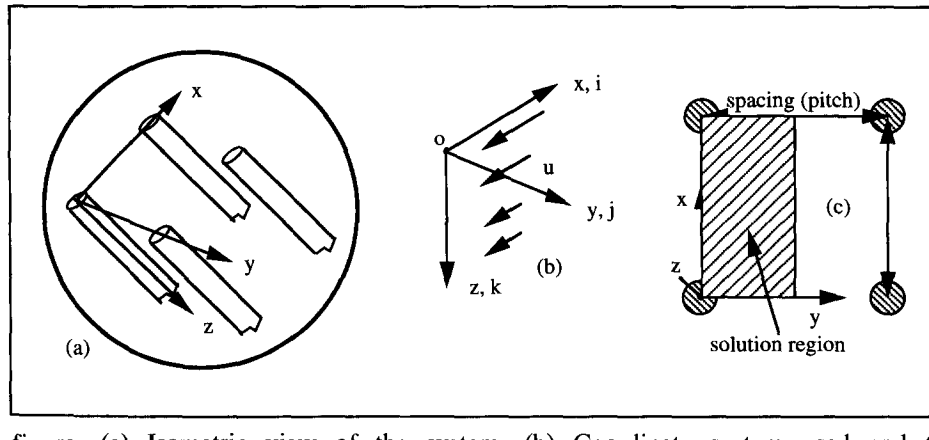

Fig. 2 Key figure. (a) Isometric view of the system, (b) Coordinate system used and the assumed displacement field, (c) Plan view of the solution region projected on to a plane parallel to the slope.

and integrating between the limits 0 to z yields the governing equation of the problem viz.;

$$G(z)\frac{\partial u}{\partial z}+\int_0^z G(\xi)\left[\frac{2(1+\nu)}{1-\nu-2\nu^2}\frac{\partial^2 u}{\partial x^2}+\frac{\partial^2 u}{\partial y^2}\right]d\xi=0 \tag{9}$$

Eq. (9) can further be simplified by introducing a linear transformation $X=\alpha x$ where:

$$\alpha=\sqrt{\frac{1-\nu-2\nu^2}{2(1+\nu)}}.$$

With this transformation Eq. (9) is reduced to the form:

$$G(z)\frac{\partial u}{\partial z}+\int_0^z \{G(\xi)\nabla^2 u\}\,d\xi=0 \tag{10}$$

where the symbol ∇^2 represent the two dimensional Laplace Operator $\frac{\partial^2}{\partial X^2}+\frac{\partial^2}{\partial y^2}$. Note that in Eq. (9) the shear modulus is not a constant but a variable as defined by Eq. (2).

Before closing this section it must be emphasized that the formulation presented here is a kinematically admissible solution in which the pertinent equation of the equilibrium is satisfied, i. e. the solution is approximate although very close to the actual solution. Also note that the governing equation must be solved with the appropriate boundary conditions which are as follow.

The boundary conditions at $y=0$ and $y=.5*s$. Let the spacing between the piles be denoted by s. In view of the symmetry of the problem it is obvious that at these boundaries;

$$\frac{\partial u}{\partial y}=0$$

for all x and all z. That is on these boundaries the conditions;

$$\frac{\partial u(x,0,z)}{\partial y}=\frac{\partial u(x,s/2,2)}{\partial y}=0$$

The boundary condition at $x=s$. This boundary represents a horizontal line passing through the tip of the piles. Again noting the symmetry it is obvious that the following condition must hold;

$$u(s,y,z)=u(0,y,z)$$

The boundary condition along the pile soil interface. The forces imposed on the pile cause a bending of the pile which causes a deflection of magnitude u_{pile}. These deflections must be equal to the displacement experienced by the soil u. Thus on this boundary the condition;

$$u_{pile}(0,r,z)=u(0,r,z)$$

where r represents the pile radius must be satisfied.

5. The numerical scheme employed

Since the governing equation is expressed in terms of $u(x, y, z)$, the soil displacement field, it

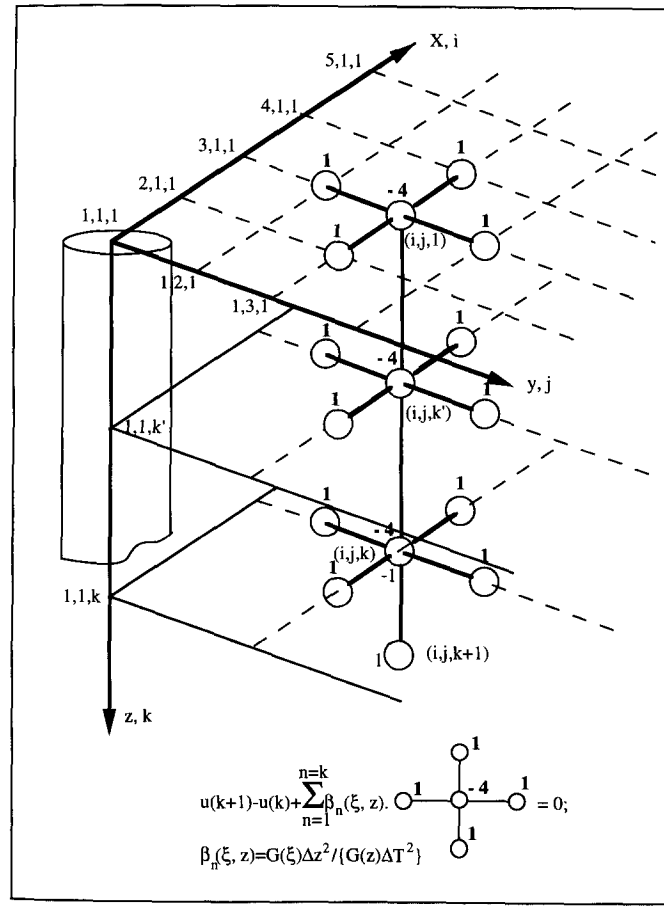

Fig. 3 The three dimensional nodal scheme used in this study.

is natural that a solution in terms of this quantity is to be sought. Thus the solution region is covered by a number of "nodal points" at which points the values of u are to be determined. Fig. 3 shows the solution region using transformed coordinates (X, y) and the proposed nodal points. To distinguish the nodes from one another each node is assigned a set of integers (i, j, k) where i=1, 2, ···, $i$max, j=1, 2, ···, $j$max and k=1, 2, ···, $k$max; $i$max, $j$max and $k$max being the maximum number in each category.

To break down the governing equation into a form suitable for numerical evaluations several steps had to be taken. First it was necessary to transfer from the (i, j, k) system to a single number to represent each node (i.e., to get the nodal number). This operation is required since the final set of equations to be solved consist of $n$max (=$i$max * $j$max * $k$max) set of linear equations to be solved for nmax set of u values; $u(1)$, $u(2)\cdots u(n\text{max})$. To achieve this transformation (from the i, j, k system to the node number, nn, system) the following equation was used.

$$nn=(k-1)\times ij\max+(i-l)\times j\max+j;$$
$$ij\max=i\max\times j\max \tag{11}$$

Next the governing Eq. (1) was broken to its finite difference form and expressed as;

$$\Delta u+\sum_{n=1}^{n=k}\beta(\xi,z)\nabla_n^2 u=0;$$

$$\beta(\xi, z)=\left[\frac{(G(\xi)\Delta z^2}{(G(z)\Delta T^2}\right] \tag{12}$$

where the operator ∇_n^2 is to operate at each level above the current point situated at level k, Δz is the interval along the z axis and $\Delta T=\Delta X=\Delta y$. The procedure of this operation is indicated at the bottom of Fig. 3.

To clarify the procedure let $i$max=6, $j$max=5 and $k$max=7 say. Then there are a total of $6\times5\times7=210$ equation to be solved for the 210 unknown nodal displacements. Furthermore let $\Delta z=.8$ and $\Delta T=1$ meters say. Now consider the node at $i=3$, $j=4$ and $k=4$ say. For this deck $z=3\times\Delta z=2.4$. According to the Eq. (11), this particular node will form equation number $nn=(4-1)\times12+(3-1)\times5+4=36+10+4=50$.

Next consider the second deck (i.e., $k'=2$). For this deck $\xi=1\times\Delta z=.8$. Thus the value of β is;

$$\beta(.8, 2.4)=\frac{G(.8)}{G(2.4)}\ \frac{.8\times.8}{1\times1}=.64\frac{G(.8)}{G(2.4)}$$

and the node on deck 2 above the nodal being considered is $(2-1)\times12+(3-1)\times5+4=26$. Thus the contribution form the nodes on deck 2 equation number 50 of the final set is;

$$\begin{aligned}
a(50, 26)u(26)&=-4\times\beta(.8, 2.4)u(26)\\
a(50, 25)u(25)&=\beta(.8, 2.4)u(25)\\
a(50, 31)u(31)&=\beta(.8, 2.4)u(31)\\
a(50, 27)u(27)&=\beta(.8, 2.4)u(27)\\
a(50, 21)u(21)&=\beta(.8, 2.4)u(21)
\end{aligned}$$

since nodes 25, 31 (=25+$j$max), 27, 21 (=26−$j$max) are the four nodes in the immediate vicinity (west, north, east and south) of node 26.

Although the procedure appears to be cumbersome, in practice it proved to be quite easy requiring a very simple subroutine.

6. Evaluations: general comments and results

In what follows three types of piles will be considered. The first type consists of timber piles of circular cross section having a Young's modulus of 1.25×10^7 kPa. The second type examined are concrete piles, again of circular cross section, having a Young's modulus of 2.94×10^7 kPa. The third type consist of Japanese steel H section with the specifications shown in Table 1 below.

Some general observations and discussions are presented first. Fig. 4 shows the behavior of a group of timber piles of various diameters and installed at several pile spacings. The depth of

Table 1 Specifications Japanese steel H piles

H×B (mm)	Area (cm^2)	Weight (kg/m)	I_{xx} (cm^4)
100×100	21.9	17.2	383
200×200	63.53	49.9	4720
300×300	119.8	94.0	20400

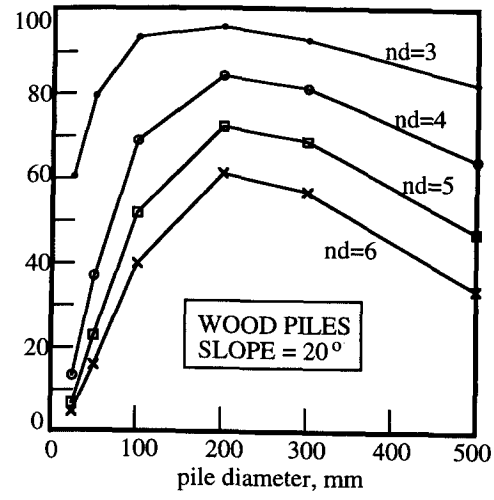

Fig. 4 Variation of efficiency with pile diameter and *nd*.

the active zone in all cases shown in the figure were taken equal to 2 meters. Note that here, and in the subsequent figures, spacing is expressed by *nd*, where *nd* stands for "multiple of diameters". Thus the actual spacing for a group of piles each 12 cm in diameter with a value of *nd*= 4 is 48 cm. Also note that the efficiency of a system, η, expressed as a percentage is defined as

$$\eta(\%) = \frac{\delta - \delta_{piled}}{\delta} \times 100$$

where δ is the creep of the untreated slope and δ_{piled} is the *maximum* creep of the slope with the piles installed. When no piles are present $\delta = \delta_{piled}$ and the efficiency is zero as expected.

From this figure it is obvious that for any given *nd* value the efficiency of the system increases with the pile diameter until it reaches an optimum value (corresponding to a pile diameter of about 200 mm) after which it drops again. The reason for this observation is simple. The value of δ_{piled}, the *maximum* creep of the slope with the piles installed, is composed of two components. The first is due to the yielding (bending) of the piles under the exerted earth pressure and the second component is caused by a movement of the soil relative to the bent piles. When the piles are "very stiff" δ_{piled} is composed almost exclusively of the second component. For "flexible piles" the reverse is true i.e., the major component contributing to δ_{piled} is the movement caused by the deformation of the piles. To demonstrate this point reference may be made to Figs. 5 and 6 which show the pattern of creep as observed on the surface of the slope and a cross section through a row of columns.

In both figures the material of the pile is wood, they both have the same diameter of 30 cm and are at the same spacing *nd*=5. In both cases the slope angle is assumed to be 20 degrees. What differentiates between the two cases is that in the first instant (shown in Fig. 5) the depth of the active zone is assumed to be one meter while in the second case (shown in Fig. 6) this depth is taken to be equal to 3 meters. In the first case the pile behaves as a rigid member as may be seen in lower part the figure and the maximum flow of the system is solely due to the creep of the surficial soils passed the piles.

The piles shown in Fig. 6, although of the same type as in the previous case are acting as flexible members (see Fig. 6b) since here the active zone is quite deep. In spite of this, the max-

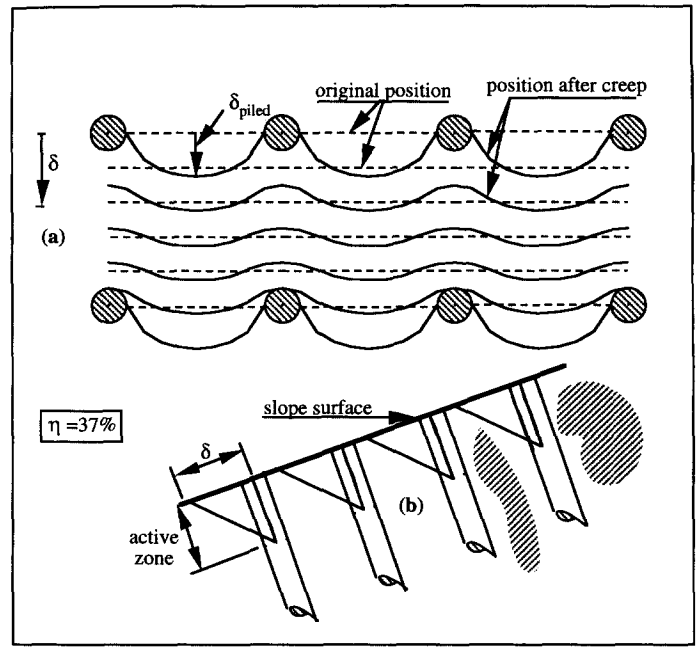

Fig. 5 Flow pattern on the slope surface (a) and mode of pile deformation (b). Active zone=1 m. Scale d on LHS=2 cm creep.

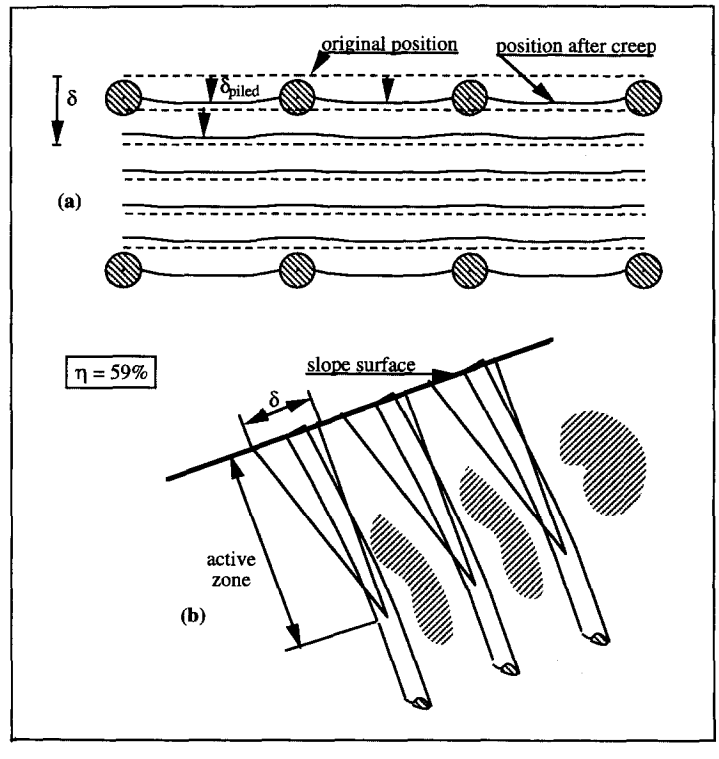

Fig. 6 Flow pattern on the slope surface (a) and mode of pile deformation (b). Active zone=3 m. Scale d on LHS=2 cm creep.

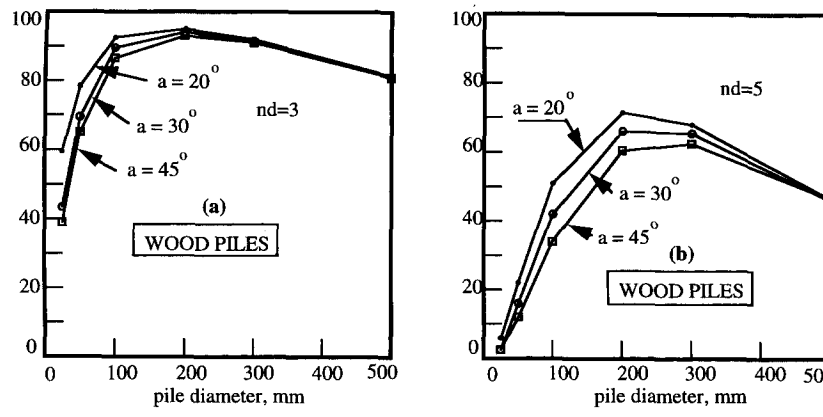

Fig. 7 Efficiency vs. spacing for various slope angles.

imum flow of the system is smaller giving rise to a higher efficiency; 59% as compared to 37% in the previous case. These two figures demonstrate clearly that the efficiency of the system is very dependent on the active zone depth.

In contrast the angle of the slope does not appear to effect the results two much. This is evi-

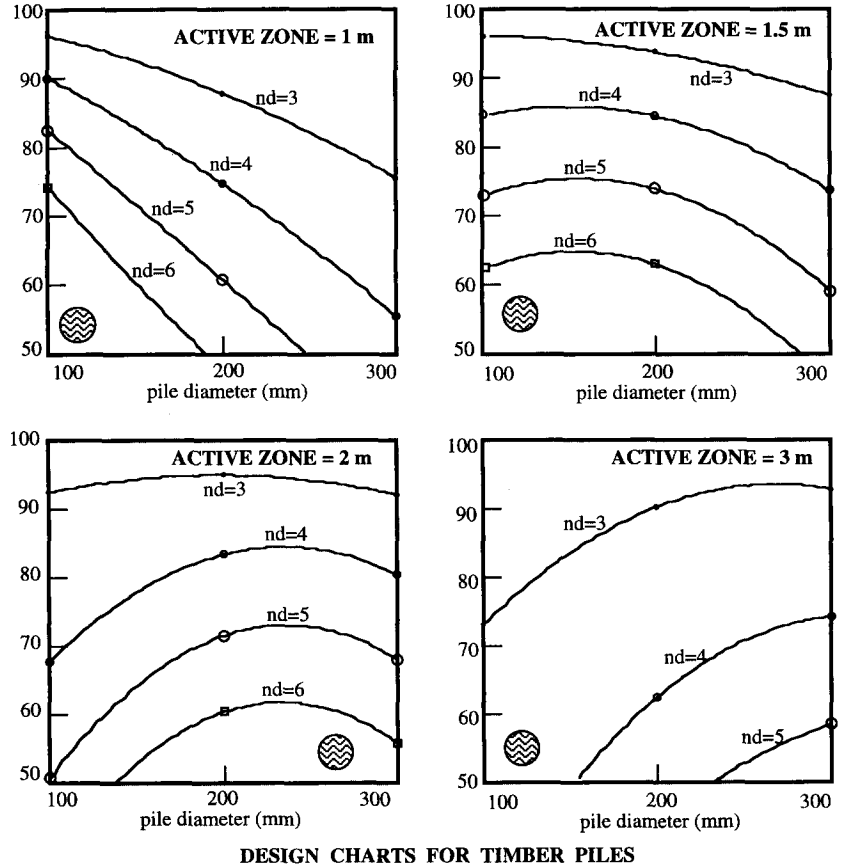

DESIGN CHARTS FOR TIMBER PILES

Fig. 8 Performance of timber piles installed at a slope of 20 degrees.

dent from Figs. 7a and 7b. Once again wood piles are used in the example and the angle of the slope is varied between 20 to 45 degrees. Note that the high value is for the sake of demonstration only: "infinite slopes" of 45 degrees in clays are very rare!

7. Evaluations: design charts

The results of the above analysis are presented in a set of three design charts which are shown in Figs. 8, 9 and 10 respectively. In all the three cases the slope is assumed to have an angle of 20 degrees and the depth of the active zone to vary between 1 meter to 3 meters as stated in the charts. Note that the efficiency values below 50% are considered low and are not indicated in the charts. The use of these charts is demonstrated by means of the following example.

7.1. Example

It is known that the depth of the active zone in a slope of 22 degrees is 2.2 meters and that the magnitude of the yearly creep is about 3 cm. Calculate the maximum creep of the system assuming concrete piles 25 cm in diameter are installed at 150 cm center to center.

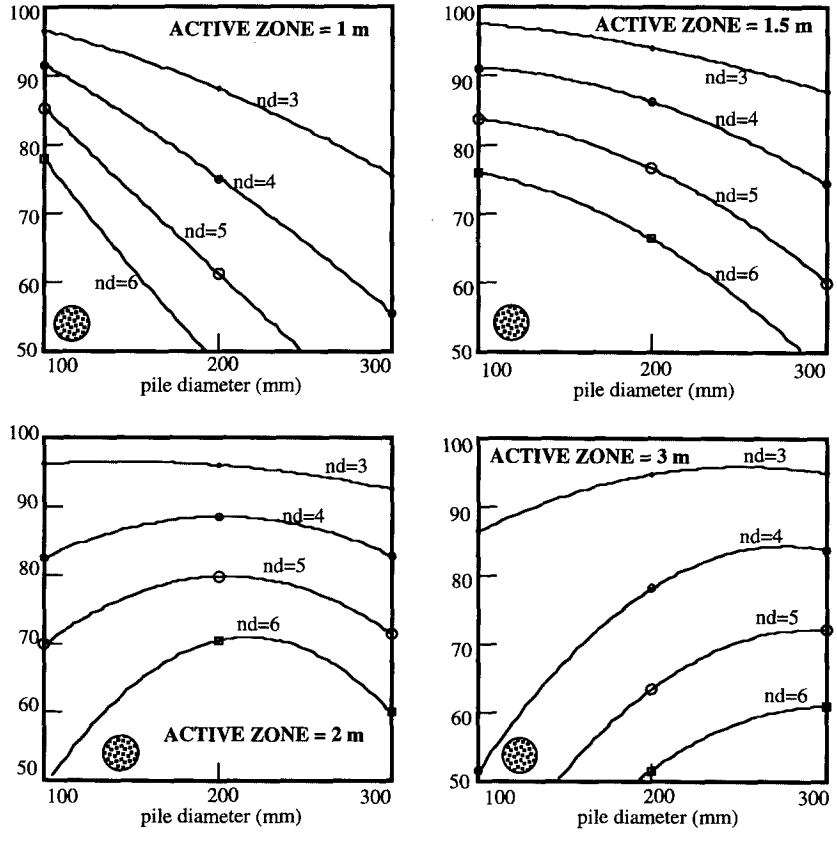

DESIGN CHARTS FOR CONCRETE PILES

Fig. 9 Performance of concrete piles installed at a slope of 20 degrees.

7.2. Solution

In this case use the chart of Fig. 9 for active zone depth 2=m. The value of *nd* is obviously 150/25=6. From the chart read the corresponding efficiency of 67%. Thus; $\delta_{piled}=\delta(1-.01\eta)=$ $3(1-0.67)=.99$. Thus the maximum creep of the piled slope is estimated to be of the order of one centimeter. It is worth noting had these piles been installed in the same pattern (spacing) and in a similar slope with an active zone depth of one meter then they would have been totally ineffective in reducing the maximum value of creep.

8. Concluding remarks

This paper merits attention for two reasons; (i) it uses a very simple method (the ID technique) in the analysis and (ii) the parameters needed for the analysis (the yearly maximum surface creep and the depth of active zone) can be measured with relative ease or they can be estimated based on the past experience. It is very unfortunate that although the technique of prevention of downhill creep using piles has been used in many locations no field results, to the knowledge of the authors, have been placed at the public domain. Thus a comparison of the results contained

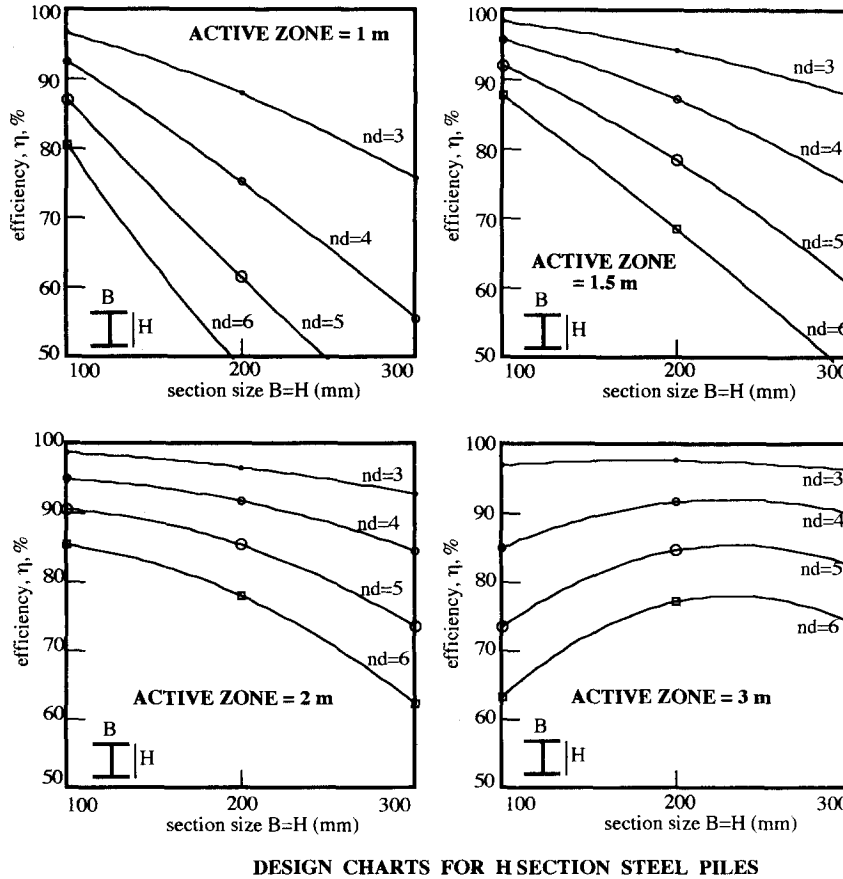

DESIGN CHARTS FOR H SECTION STEEL PILES

Fig. 10 Performance of H section steel piles installed at a slope of 20 degrees.

in the paper with actual field records is not possible at this stage. It is also important to realize that the analysis is applicable to formations which undergo successive drying and wetting i.e., locations where the surficial soils are unsaturated for a good period of the year.

Next, a comment about the physical properties (constitutive constants) describing material behavior as used in the analysis. The use of symbol G_w and G_d Eqs. (1) to (3) to describe the shear stress-strain characteristic of the soil does not mean that the soil is treated as an elastic material. Only that the soil within the range of strains encountered (of the order of 1%) behaves linearly which is a good approximation. Elasticity implies reversibility and of course no such claim is made. Furthermore for an elastic solution the shear modulus is kept constant throughout. In the analysis presented here it is linearly varying from a small value near the surface to its maximum value at the depth corresponding to the depth of the active zone. In this respect and within the active zone the material is assumed to behave as a Gibson Foundation, a concept widely used in geotechnical analysis.

Acknowledgements

The financial support received from the Natural Science and Engineering Council of Canada and the Institute for Lowland Technology of Saga University, Japan in support of this work is gratefully acknowledged.

References

Fukuoka, M. (1977), "The effect of horizontal loads on piles due to landslides", *Proc. 9th ICOSMFE*, Tokyo, Spec. Session 10.

Gassler, G. (1990), "In-situ technique for reinforced soil. State of the art lecture", *Proc. Int. Reinforced Soil* Con., Glasgow, Scotland, 185-196, Thomas Telford, London

Gudehus, G. and Schwarz, W. (1981), "Stabilization of creeping slopes by dowels", *Proc. 11th ICOSMFE, Stockholm*, **3**, 1697-1700.

Ito, T. and Matsui, T. (1975), "Methods to estimate lateral forces on stabilizing piles", *Soil and Foundations*, **15**(4), 45-59.

Pearlman, S.L., Campbell, B.D. and William, J.L. (1992), "Slope stabilization using in-situ earth reinforcement", *Proc. ASCE Conf. on Stability and performance of slopes and embankments-A 25 year perspective*, The University of California, 1333-48.

Poorooshasb, H.B. Azevedo, R. and Ghavami, K. (1980), "Analysis of slopes with bamboo dowels", *Proc. Intl. Geotch. Symp.*, Theory and Practice of Earth Reinforcement, Fukuoka, Japan, Yamanouchi, Miura and Ochiai, Editors, pp. 467-472.

Poorooshasb, H.B., Alamgir, M. and Miura, N. (1996), "Application of an integro-differential equation to the solution of geotechnical problems", to appear in the journal *Structural Engineering and Mechanics*.

Poorooshasb, H.B., Miura, N. and Alamgir, M. (1996), "Refinement of a numerical technique for solution of geotechnical problems", *3rd Asian-Pacific Conference on Computational Mechanics*, 16-18 September 1996, Seoul, Korea.

Reese, L.C., Wang, S.T. and Fouse, J.L. (1992), "Use of drilled shafts in stabilizing a slope", *Proc. ASCE Conf. on Stability and performance of slopes and embankments-A 25 year perspective*, The University of California, pp. 1318-32.

Viggianti, C. (1981), "Ultimate lateral load on piles used to stabilize landslides", *Proc. l0th ICOSMFE*, Stockholm, 555-560.

Wang, W.L. and Yen, B.C. (1974), "Soil arching in slopes", *ASCE J. GE Div.*, **100**, GTl, Jan. 1974.